Chapter 1

Low frequency seismology and three-dimensional structure — observational aspects

Guy Masters and Michael Ritzwoller

The availability of a large quantity of long period digital seismic data has played a major role in recent advances in our understanding of the large scale aspherical structure of the Earth. Many new models exist which have been designed to fit these data. They succeed to various degrees but it is indisputable that much of the signal in the data remains to be explained.

We illustrate the kinds of signals that models of aspherical structure should reproduce and then indicate the theoretical framework in which these observations may be interpreted. Finally, we discuss the "first generation" of aspherical Earth models which demonstrate that we need to be more sophisticated in our interpretative techniques if we are to obtain consistent models of structure.

1. Introduction

If the Earth were truly spherically symmetric, it is probably fair to say that the low frequency seismologist would now be out of business. Compact expressions for an observed seismogram on a spherical Earth as a sum of decaying cosinusoids have been around since the early 1970s (Gilbert, 1970). Array processing techniques based on this theory were introduced in the mid 1970s and were successfully applied to hand-digitized data (Gilbert and Dziewonski, 1975). With the vast improvement in the quantity and quality of digital data since that time, one might reasonably expect that we would, by now, fully understand the long period spectrum of seismic motion. Needless to say, this has not

N.J. Vlaar, G. Nolet, M.J.R. Wortel & S.A.P.L. Cloetingh (eds), Mathematical Geophysics, 1-30.

happened. Better data and more sophisticated ways of processing them have revealed a plethora of signals that cannot be modeled by spherically symmetric structure alone. The main purpose of this paper is to acquaint the reader with the types of signals that the low frequency seismologist is now trying to explain. Some of the signals are unsurprising, e.g., the effect of rotation of the Earth on the longest period part of the spectrum has been observed and understood for over 25 years (Backus and Gilbert, 1961; Pekeris et al., 1961; Ness et al., 1961; Benioff et al., 1961). Others are completely unexpected and, as of the time of writing, unexplained.

The complexities in the low frequency spectrum arise because rotation and lateral structure remove the spherical symmetry. On a spherically symmetric Earth, modes of oscillations would be degenerate, i.e., a group of modes or "singlets" would have the same frequency. Such groups of singlets are called "multiplets." The removal of spherical symmetry completely removes the degeneracy so that each singlet within a multiplet has a slightly different frequency. This "splitting" dominantly affects spectra by producing phase shifts relative to the spherically symmetric reference state. Coupling between singlets, either within a multiplet or between multiplets, can also produce further phase and amplitude perturbations. These effects are now observationally well documented and are slowly becoming better understood.

The next section of this paper gives a brief look at the low frequency digital data and attempts to highlight some of the observational problems we encounter. This is followed by an overview of the theoretical background required to model the data and we close with an evaluation of some recently proposed three-dimensional models.

2. Long period data

The main sources of long period data are the IDA array (Agnew et al., 1976, 1986), the SRO and ASRO components (Peterson et al., 1980) of the Global Digital Seismic Network (GDSN) and, more recently, GEOSCOPE (Romanowicz et al., 1984). The original IDA instrumentation consists of an electrostatically fed-back Lacoste-Romberg gravimeter. Electrostatic feedback has the disadvantage of being relatively weak but has the advantage that only modest amplification is needed to get a usable signal. (The development of low noise electronic amplifiers has allowed the use of electromagnetic feedback which is capable of a much larger force.) The IDA instruments are therefore susceptible to signal distortion of the early part of recordings of large events and the first Rayleigh wave is usually lost for events greater than $M_S = 6.5$. Nevertheless, we are usually interested in many hours of recording for free oscillation work so the loss of the initial part of the record is not as severe as it might seem. Another drawback of the IDA data is that only the vertical component is recorded. Many modes of oscillation are dominantly horizontally polarized so three component recording is desirable. This led to the use of the SRO and ASRO components of the GDSN. The difficulty of making long time series from SRO data has meant that few investigators have used this data source though useful signal exists to periods longer than 500 seconds for the largest events. Figure 1 shows the acceleration response of several seismic systems. The ASRO system has a long period response intermediate between the IDA and SRO systems. Note the very poor low frequency response of the DWWSSN and RSTN components of the GDSN. The DWWSSN is also extremely noisy so neither the DWWSSN nor RSTN system have seen much use in very

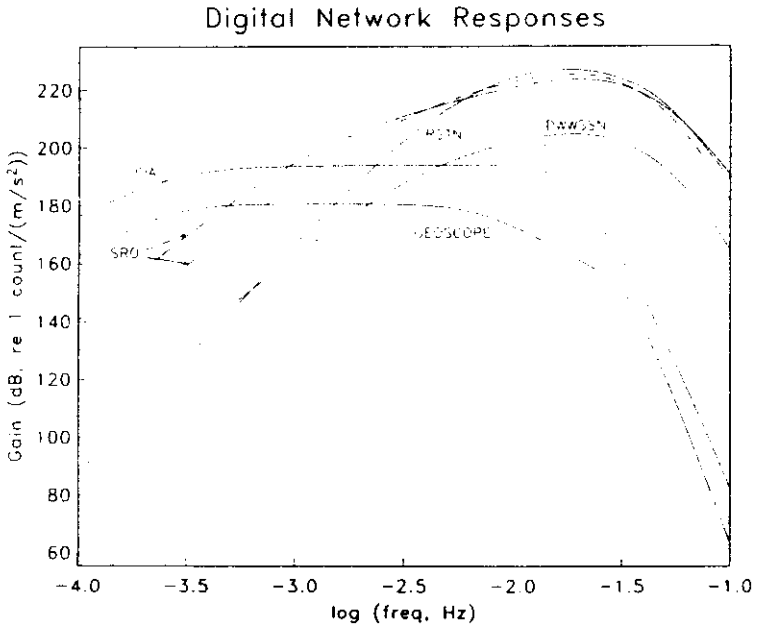

Figure 1. Response to acceleration of some currently operating global digital networks. The long period channels of the components of the GDSN are shown (i.e., SRO, RSTN, and DWWSSN). The mode channel for IDA and the very long period channel for GEOSCOPE are also shown. Recent modification of the SRO has resulted in an improved long period response.

long period seismology. Even the SRO and ASRO networks were not initially designed for long period work and so calibration of the long periods is relatively poor. It appears that calibration signals provided with the data are not reliable enough to constrain the very long period response. This leads to difficulties when performing analyses which mix GDSN and IDA data. New sensor and electronics design have led to improvements in long period instrumentation (Wielandt and Streckheisen, 1982) and new arrays (e.g., GEOSCOPE) are now providing easy to use, high quality three component long period data. Upgrading of WWSSN and IDA stations will hopefully soon result in a large, high quality global network.

Figure 2 shows some typical waveforms from the IDA, SRO and ASRO networks which have been filtered so that only periods longer than 150 seconds are visible. Also shown are synthetic seismograms constructed for a spherically symmetric Earth model. While visual agreement is very good there are many details which are not modeled and which provide strong constraints on aspherical structure. Figure 3 shows some Fourier amplitude spectra of Hanning tapered recordings. The fundamental mode oscillations are clearly visible along with some lower amplitude overtones. Note that individual mode peak amplitudes are quite poorly predicted by the spherical Earth synthetics even though the time domain fits of Figure 2 are very good. These examples are for events with moments of about 10^{27} dyne cm and signal with periods in excess of 750 seconds is clearly visible. We primarily look at the data in the frequency domain so the method of estimating the Fourier spectra merits some discussion. Until recently, a direct estimate using a single, *ad-hoc* data window has been the method of choice. Different windows give different

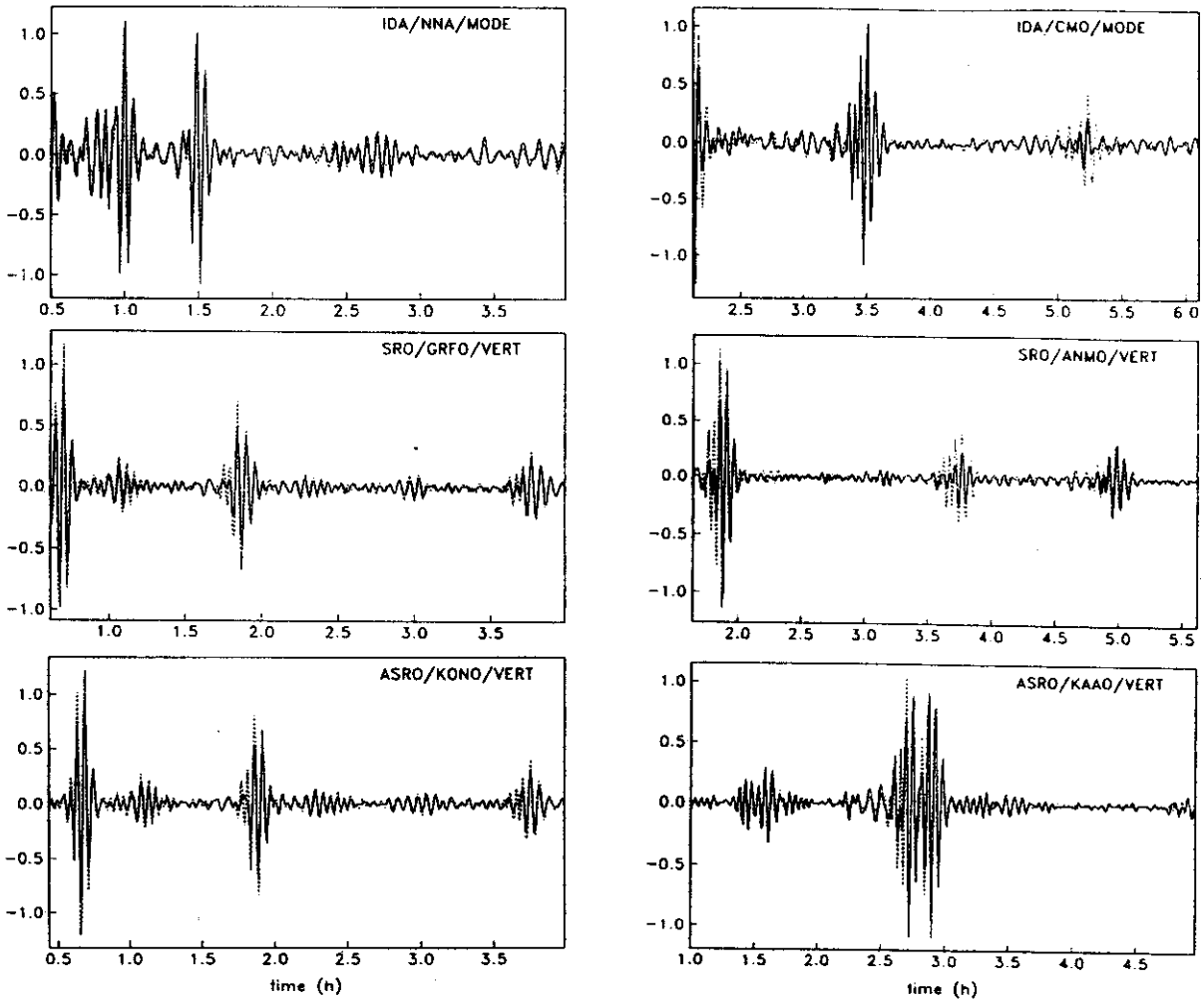

Figure 2a (left panel). A comparison of long period waveforms (T>150 secs) with spherical Earth synthetic seismograms for a) a large, deep event (Banda Sea 1982/173). Examples for the IDA, SRO and ASRO networks are shown. Note that fundamental mode Rayleigh wave packets dominate even the recordings of very deep events.
Figure 2b (right panel). As for Figure 2a except for a large shallow event (Iran 1978/259).

compromises between resolution and spectral leakage and we show the effect of several different data windows in Figure 4. If we have a harmonic signal in noise, it is possible to find a taper which minimizes spectral leakage for a particular resolution width. Such tapers are relatively easy to calculate (Slepian, 1978) and are called "discrete prolate spheroidal sequences" (or just "prolate windows"). For our example in Figure 4, the 2π prolate window gives a reasonable compromise between peak width and side band level. The familiar Hanning window gives similar results and is, of course, much easier to compute and so has seen the most usage. The Blackman-Harris 4-term taper (Harris, 1978) gives similar results to the 4π prolate window but the peaks are sufficiently broadened that spectral details are lost. (On the other hand spectral leakage is almost negligible.) We need not limit ourselves to one taper as families of tapers can be constructed for a given resolution width. These have progressively worsening spectral leakage properties but the

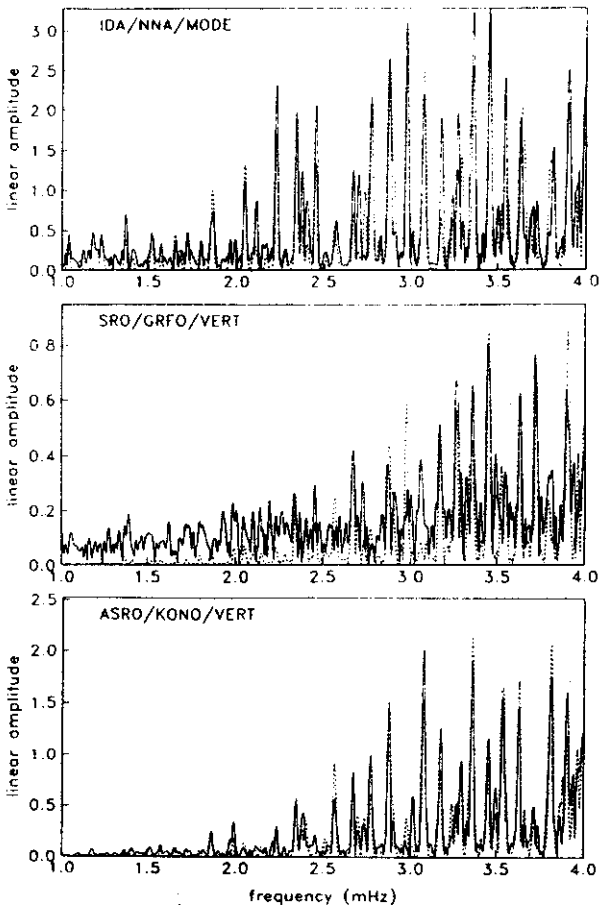

Figure 3. Spectra of 30-hour recordings in the frequency band 1 to 4 mHz. The recordings have been Hanning tapered to reduce spectral leakage. Examples from the IDA, SRO and ASRO networks are shown. The SRO instruments are generally of slightly inferior quality in this frequency band. The dashed lines are spectra of spherical Earth model synthetic seismograms. Note that the detailed fit in the frequency domain looks quite poor despite the excellent fit in the time domain (Figure 2a).

first few can be used to obtain useful spectral estimates. This multiple-taper method has been described by Thomson (1982) and extended for use with decaying sinusoids by Lindberg (1986). The method allows reliable line detection and it may be possible to detect low signal spectral lines that would otherwise be missed. Multiple-taper analyses are relatively new so examples presented in the remaining part of this section will use only the Hanning taper. It is clearly apparent from Figure 4 that some taper must be used as the distortion due to spectral leakage in the absence of a taper is sufficient to give grossly erroneous estimates of center frequencies, apparent attenuation, etc. Further discussion of this point can be found in Dahlen (1982) and Masters and Gilbert (1983).

As noted in the introduction, departures of the Earth from sphericity lead to splitting and coupling of free oscillations. These effects manifest themselves in the data in a variety of ways. At the lowest frequencies, the rotation of the Earth causes strong splitting of modes of oscillation (Figure 5) and leads dominantly to a linear distribution of the singlet frequencies in azimuthal order. The rotational bulge of the Earth is an axisymmetric

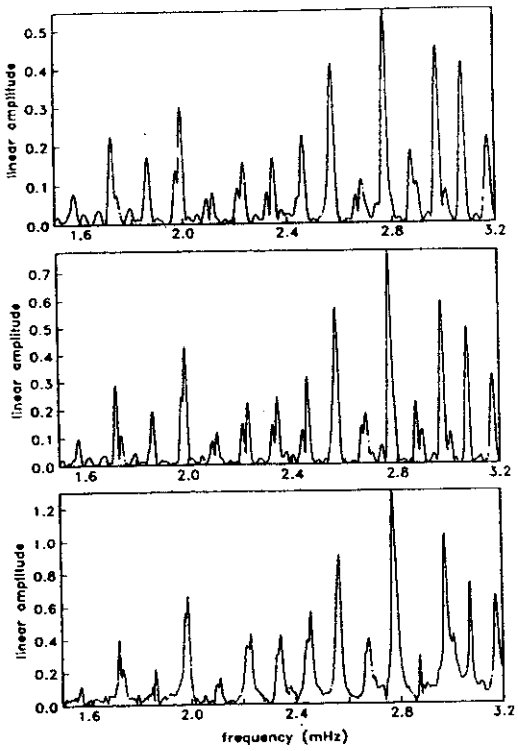

Figure 4. Direct spectral estimates of a 35-hour time series using a boxcar taper (lower panel), a 2π prolate (middle panel) and a 4π prolate (upper panel). In the lower panel, the distortion caused by spectral leakage is so great that the spectral estimate using a boxcar taper is useless. In the upper panel the peak widths are so broad that some multiplets appear to overlap. The 2π prolate gives a reasonable compromise between resolution and spectral leakage.

feature which is dominated by harmonic degree 2 and leads to a parabolic distribution of singlet frequencies. The joint effect is a quadratic in azimuthal order (Dahlen, 1968). Careful processing of many records allows the individual singlets to be isolated (see below) and the results are often in good agreement with the predictions of a rotating Earth in hydrostatic equilibrium. For many modes (in particular high Q, low l modes which sample into the Earth's core), the rotating, hydrostatic Earth model explains little of the observed signal. Some modes can have singlets distributed over a frequency band up to two and a half times greater than theoretically predicted (Figure 6). This "anomalous splitting" of modes suggests the presence of deep seated large scale aspherical structure and will be discussed further below.

As one goes to higher frequency, higher l modes it is impossible to directly observe splitting as in the above examples and a multiplet may often appear to be a single resonance function. In fact, the model of a single decaying cosinusoid can usually explain the observations though the inferred center frequency and attenuation rate vary from recording to recording (Figure 7). A discussion of the many methods that can be used for estimating frequencies and attenuation rates can be found in Masters and Gilbert (1983). In practice the techniques require the use of high signal spectral peaks that can be unambiguously

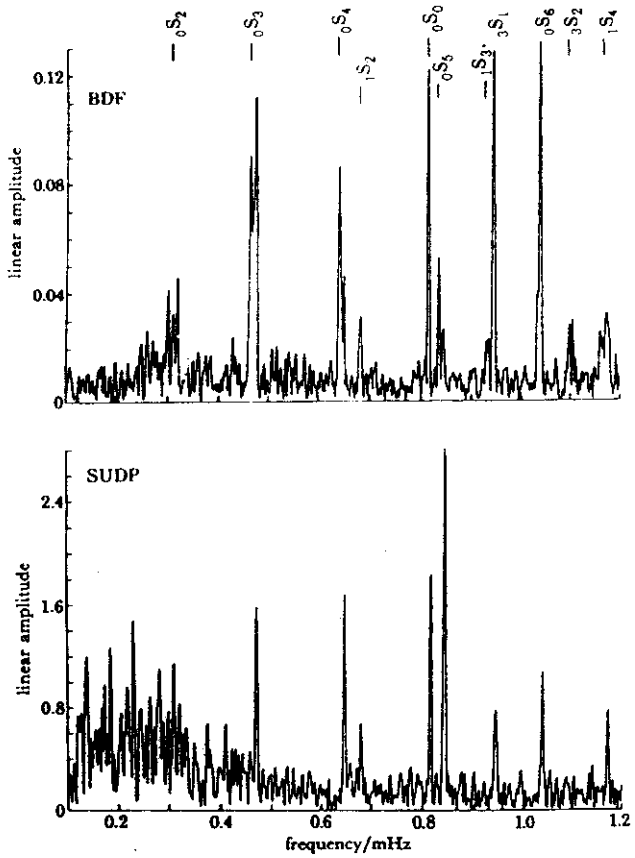

Figure 5. Two spectra of 120-hr records from the Sumbawa earthquake of 1977. In the upper panel, the effects of rotation and ellipticity cause obvious splitting at the IDA station at Brasilia. In the lower panel, the spectrum of the UCLA South Pole recording shows no obvious splitting though it is noisy at frequencies below 0.4 mHz. The lack of splitting at a pole is to be expected if rotation and axisymmetric aspherical structure are the dominant perturbing influences.

identified so the analysis of single recordings by this method is mainly limited to periods longer than about 150 seconds and to the highly excited fundamental modes. Some high Q overtones can be analyzed by using the Earth as an attenuation filter, i.e., the data window used in spectral estimation is started several hours after the origin time of the event so that low Q modes have been significantly attenuated.

The effects of splitting of a multiplet in the low frequency spectra are obvious. More subtle is the effect of multiplet/multiplet coupling. Detection of such coupling is often difficult as closely spaced multiplets may or may not be coupled depending upon the nature of aspherical structure. One type of coupling which will obviously be present is Coriolis coupling between ${}_0S_l$ and ${}_0T_{l\pm1}$ multiplets if they are sufficiently close in complex frequency (Dahlen, 1969; Luh, 1973, 1974; Woodhouse, 1980; Masters et al., 1983; Fichler et al., 1986). Conditions for observable amounts of Coriolis coupling actually exist for ${}_0S_8/{}_0T_9$ through ${}_0S_{22}/{}_0T_{23}$ (a frequency range of 1.7 to 3.1 mHz). This coupling means that we observe spectral lines which are hybrid spheroidal/toroidal motion and thus spectral

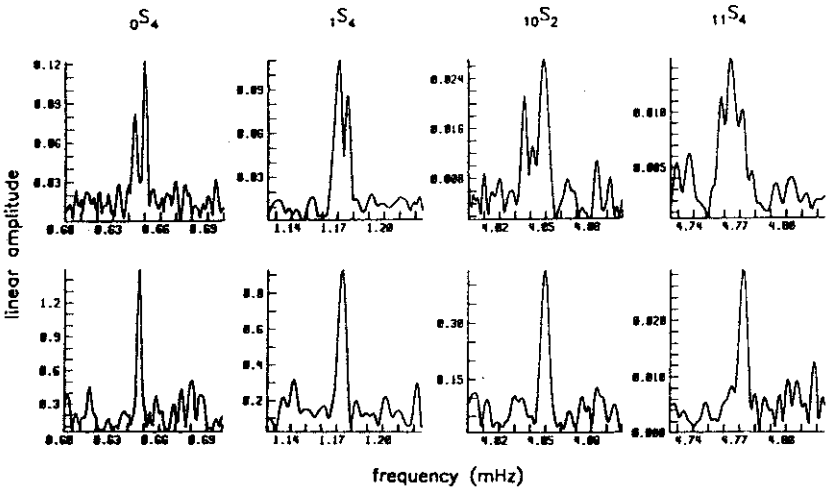

Figure 6. Detailed spectra of four low harmonic degree multiplets recorded at nonpolar latitudes (upper figures) and polar latitudes (lower figures). Each nonpolar spectrum shows clear evidence of splitting though the polar spectra are not obviously split. This is surprising for $_{10}S_2$ and $_{11}S_4$ as they are insensitive to the rotation of the Earth. These latter two modes sample into the core and are very strongly split. They both span frequency bands in excess of 13 μHz though are predicted to be less than 7 μHz wide for a rotating hydrostatic Earth.

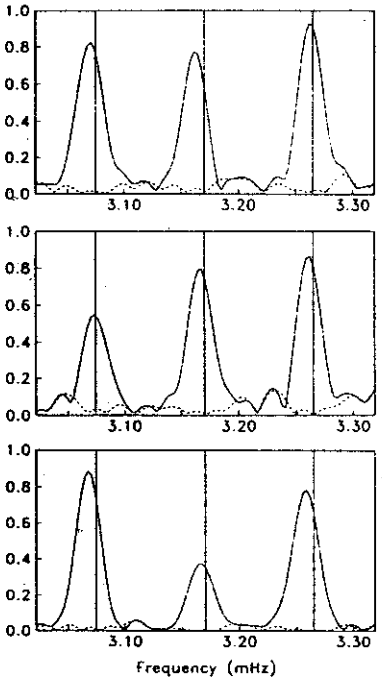

Figure 7. Linear amplitude spectra of a frequency band encompassing the fundamental modes $_0S_{22} \rightarrow {}_0S_{24}$. The solid line is the original spectrum while the dashed line is the residual after the best fitting decaying cosinusoid model has been fit to the data. The data are for the Iran 1978/259 event recorded at CMO (top), HAL (middle), and PFO (bottom). Also shown are the theoretical degenerate multiplet frequencies predicted by Model 1066A. A decaying cosinusoid is a good model for the data though the apparent center frequencies are quite variable.

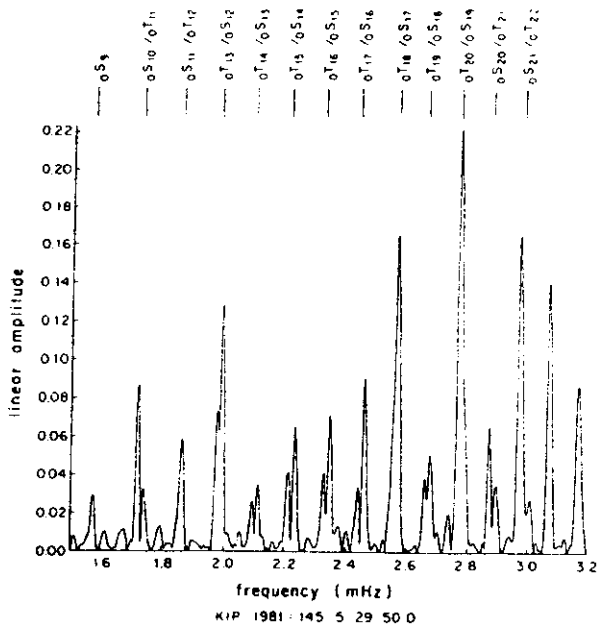

Figure 8. A 35-hour Hanning-tapered spectrum of a vertical component recording made at KIP of an event south of New Zealand 1981/145. The source mechanism of this event was particularly good at exciting toroidal modes and the Coriolis coupling of these modes to nearby spheroidal modes is particularly obvious.

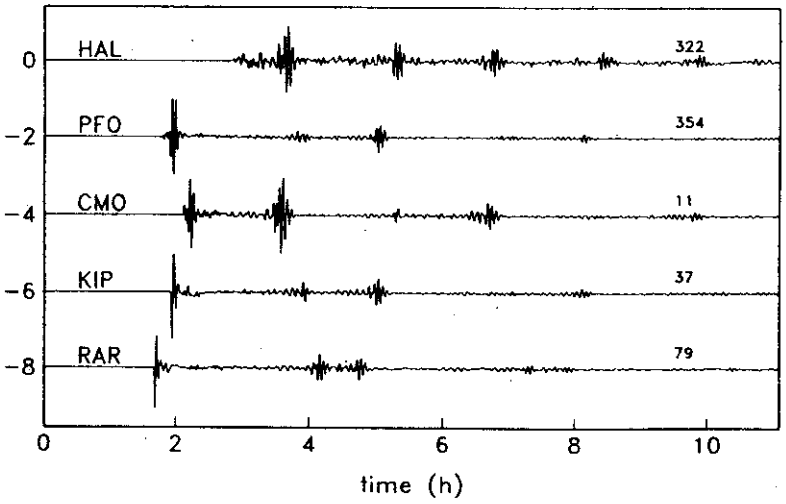

Figure 9. IDA recordings of the Iran 1978/259 event low passed so that only periods of 150 sec or longer are visible. The numbers on the right are the azimuths to each receiver in degrees. Note that PFO, CMO and KIP are all at a very similar azimuth but show very different Rayleigh wave amplitude behavior. This example of surface wave amplitude anomalies was first discussed by Niazi and Kanamori (1981)

peaks can occur on vertical component recordings near the frequencies of toroidal modes. An example of this is shown in Figure 8 where a whole suite of spectral peaks near toroidal mode frequencies can be seen. On vertical component recordings, two clumps of energy are visible with one (closest to the original uncoupled spheroidal mode) being dominant. If

the properties of this spectral peak are interpreted as being those of an uncoupled spheroidal mode then significant bias can result. For example, the mean frequency of a dominantly spheroidal hybrid mode can be two or three microhertz from the true spheroidal mode frequency. This constitutes a bias of several standard deviations. Apparent attenuation rates are similarly affected. Another form of coupling which should also provide measurable signals is so called "along-branch" coupling; e.g., the coupling of ${}_0S_l$ to ${}_0S_{l\pm1}$ modes. This coupling provides some sensitivity to odd-order structure (see below) and is therefore of great interest. Because of the relatively large frequency spacing of fundamental modes (~100 μHz), this kind of coupling causes only a weak signal which cannot be illustrated by direct inspection of the spectrum. It may be more apparent in the time domain where the expected effect of coupling between neighboring fundamental modes is to produce a phase shifted wave packet though theoretical calculations with existing models of long wavelength structure show that the effect is small (Park, 1986).

Inspection of the time domain fits of spherical Earth point source synthetic seismograms to data often reveals large surface wave amplitude anomalies. These anomalies are most apparent when a Rayleigh wave packet R_n is smaller than the next packet, R_{n+1} (Figure 9). For the largest events, it is possible that some of the observed anomaly is due to source finiteness. A more likely cause is a focusing/defocusing effect of aspherical structure (Lay and Kanamori, 1985; Woodhouse and Wong, 1986). The amplitude anomalies are visible for nearly every event, regardless of size, which makes an explanation based on source finiteness untenable.

At periods shorter than about 150 seconds, it is extremely difficult to identify individual peaks in the spectra of single recordings and it becomes more natural to work in the time domain. (Note that stacking of the spectra of many recordings still allows individual modes to be identified at much higher frequencies.) Individual surface wave packets consisting dominantly of fundamental modes can be isolated in the data and great circle or single station phase velocity or group velocity measurements performed (see, e.g., Nakanishi and Anderson, 1983, 1984). Great circle phase velocity analysis reduces basically to a transfer function estimation problem for mapping R_n into R_{n+2} and several quite sophisticated techniques have been developed to do this (e.g., Nakanishi, 1979). Unfortunately the analysis is restricted to relatively short data lengths so that the transfer function at periods longer than 250 secs is unreliable. Traditional transfer function estimation techniques use frequency domain averaging to estimate errors (e.g., Jenkins and Watts, 1968) though we are unaware of a formal error analysis in a seismological context. Single station measurements are much more difficult to perform and require corrections for source mechanism, instrumental response and higher mode contamination and are also sensitive to errors in epicenter location. These difficulties have led some authors to abandon the estimation of intermediate quantities from the data and to directly model waveforms in terms of Earth structure (Dziewonski and Steim, 1982; Woodhouse and Dziewonski, 1984; Tanimoto, 1987). This is intuitively very satisfying but suffers from some practical drawbacks. Perhaps the most contentious problem is the assessment of goodness of fit and the consequent determination of errors on the model parameters. Assigning an "error" to a waveform is not a trivial task.

Returning to the main theme of this section, i.e., the signal from aspherical structure, we can summarize as follows. Low frequency time series are dominated by fundamental

mode energy (even for very deep events). In the frequency domain, the spectral peaks of fundamental modes are clearly shifted or observably split and individual peak amplitudes are not well fit by spherical Earth synthetics. A consequence of the splitting is that measured Q values are extremely variable. We can also observe Coriolis coupling of toroidal/spheroidal multiplets. In the time domain we observe phase shifting of surface wave packets and strong amplitude anomalies. If we use extremely long records we can enhance high Q overtones relative to the low Q fundamental modes and the spectra of many of these overtones show strong anomalous splitting.

3. Theoretical review

We consider first the case of uncoupled multiplets. A complete description of the seismogram of an uncoupled multiplet on a slightly aspherical Earth is given by Woodhouse and Dahlen (1978) and by Woodhouse and Girnius (1982). We summarize the results for the kth multiplet where k is shorthand for (n, l, q) where n is the radial order, l the harmonic degree, and q the mode type (spheroidal or toroidal).

A component of the displacement field at position $\mathbf{r}=(r,\theta,\phi)$ excited by a point source at $\mathbf{r}_0$ with moment rate tensor $\mathbf{M}$ can be written as the inner product

$$s(\mathbf{r},t)=\mathrm{Re}\left\{\sum_k \boldsymbol{\sigma}_k^T(\mathbf{r})\cdot\mathbf{a}_k(\mathbf{r}_0,t)e^{i\omega_k t}\right\} \tag{1}$$

where the complex envelope function vector $\mathbf{a}_k(t)$ is given by

$$\mathbf{a}_k(t)=\mathbf{P}_k(t)\mathbf{a}_k\,,\quad \mathbf{a}_k(0)=\mathbf{a}_k \tag{2}$$

$\mathbf{P}_k(t)=\exp(i\mathbf{H}_k t)$ is the matrizant or propagator matrix of the following first-order propagator equation with initial condition given in (2):

$$\frac{d}{dt}\mathbf{a}_k(t)=i\mathbf{H}_k\mathbf{a}_k(t) \tag{3}$$

The receiver vector $\boldsymbol{\sigma}_k$ in (1) is composed of the $2l+1$ singlet eigenfunctions:

$$\boldsymbol{\sigma}_k^m(r)=[\hat{\mathbf{r}}U_k(r)Y_l^m(\theta,\phi)+V_k(r)\nabla_1 Y_l^m(\theta,\phi)-W_k(r)\hat{\mathbf{r}}\times\nabla_1 Y_l^m(\theta,\phi)]\cdot\hat{\mathbf{n}} \tag{4}$$

where $\nabla_1=\hat{\boldsymbol{\theta}}\partial_\theta+(\sin\phi)^{-1}\hat{\boldsymbol{\phi}}\partial_\phi$ and where the unit vector $\hat{\mathbf{n}}$ determines which component is represented by s in (1).

The excitation vector $\mathbf{a}_k$ comprises the $2l+1$ excitation coefficients $a_k^m=\mathbf{M}:\boldsymbol{\varepsilon}_k^{m*}(\mathbf{r}_0)$. The term $\boldsymbol{\varepsilon}_k^{m*}$ is the complex conjugate of the strain tensor for the azimuthal order m singlet and is expressible in terms of the multiplet scalars U_k, V_k, and W_k in (4) (Gilbert and Dziewonski, 1975). The complex spherical harmonics, Y_l^m, are normalized according to the convention of Edmonds (1960).

The dependence of displacement on aspherical structure in (1) can be made explicit by considering the components of the $(2l+1)\times(2l+1)$ complex splitting matrix $\mathbf{H}_k$:

$$H_{mm'}^k=\omega_k(a_k+mb_k+m^2c_k)\delta_{mm'}+\sum_{\substack{s=2\\ \text{even}}}^{2l}\gamma_s^{mm'}{}_k\,c_s^{m-m'} \tag{5}$$

where

$$ {}_k c_s^t = \int_0^a \delta \mathbf{m}_s^t(r) \cdot {}_k \mathbf{G}_s(r) r^2 dr - \sum_d^D r_d^2 h_{sd}^t \, {}_k B_s \tag{6} $$

The first term on the right hand side of (5) represents the contribution by rotation and hydrostatic ellipticity of figure. Here ω_k is the degenerate frequency and numerical values of the splitting parameters a_k, b_k, and c_k evaluated for some multiplets can be found in Dahlen and Sailor (1979) and Ritzwoller et al. (1986). We call the model containing only these contributions to $\mathbf{H}_k$ the RH model (standing for rotating, hydrostatic earth model). The second term contains the additional effect of general even-order aspherical volumetric ($\delta \mathbf{m}_s^t(r)$) and boundary (h_{sd}^t) perturbations. Aspherical perturbations are represented with spherical harmonic basis functions of degree s and order t:

$$ \delta \mathbf{m}(\mathbf{r}) = \sum_{s,t} \delta \mathbf{m}_s^t(r) Y_s^t(\theta, \phi) \qquad h_d(\theta, \phi) = \sum_{s,t} h_{sd}^t Y_s^t(\theta, \phi) \tag{7} $$

for each boundary d. The model vector is

$$ \delta \mathbf{m}_s^t(r) = (\delta \rho_s^t(r), \delta \kappa_s^t(r), \delta \mu_s^t(r))^T $$

and the integral kernel vector is

$$ \mathbf{G}_s(r) = (R_s(r), K_s(r), M_s(r))^T $$

where R_s, K_s, and M_s can be computed using the formulas given by Woodhouse and Dahlen (1978). Each multiplet k possesses a unique set of complex structure coefficients ${}_k c_s^t$ whose amplitude and phase are functions of the amount and distribution of heterogeneity in the earth and of the manner in which the multiplet samples this heterogeneity. The γ function in equation (5) can be written in terms of Wigner $3j$ symbols which may be computed using the recurrence relations given by Schulten and Gordon (1975). Thus, estimation of the c_s^t fully determines the splitting matrix. Note that, for an isolated multiplet, only those components of $\delta \mathbf{m}$ with s even contribute to the splitting matrix. Coupling between nearby multiplets can give some sensitivity to odd-order structure but the coupling is usually weak so that low frequency seismograms are dominantly sensitive only to even-order structure. This fact should be borne in mind when looking at models of aspherical structure derived from low frequency data.

Insight into the way aspherical structure affects the displacement field is gained by considering the spectral decomposition of $\mathbf{H}_k$:

$$ \mathbf{H}_k \mathbf{U}_k = \mathbf{U}_k \boldsymbol{\Omega}_k \tag{8} $$

Here $\mathbf{U}_k$ is the unitary matrix whose columns are the eigenvectors of $\mathbf{H}_k$ and $\Omega_{mm'}^k = \delta \omega_k^m \delta_{mm'}$ is the diagonal matrix of eigenvalues. Equation (1) can then be written as

$$
\begin{aligned}
s(\mathbf{r},t) &= \mathrm{Re}\left\{ \sum_k \boldsymbol{\sigma}_k^T(\mathbf{r}) e^{i\mathbf{H}_k t} \mathbf{a}_k(\mathbf{r}_0,0) e^{i\omega_k t} \right\} \\
&= \mathrm{Re}\left\{ \sum_k (\boldsymbol{\sigma}_k^T \mathbf{U}_k) e^{i(\boldsymbol{\Omega}_k+\omega_k)t} (\mathbf{U}_k^{-1}\mathbf{a}_k(\mathbf{r}_0,0)) \right\}
\end{aligned}
\tag{9}
$$

Equation (9) demonstrates that aspherical structure splits the singlet frequencies within each multiplet: $\omega_k^m = \omega_k + \delta\omega_k^m$. For the RH model, $\omega_k^m = \omega_k + \omega_k(a_k + mb_k + m^2 c_k)$ and $\mathbf{U}_k = \mathbf{I}$. If $\mathbf{U}_k = \mathbf{I}$, the mth singlet frequency is uniquely associated with the mth element of the receiver and excitation vectors. In this case, each envelope function $a_k^m(t)$ in (1) is a pure harmonic time function. Additional aspherical structure further splits the singlet frequencies and perturbs $\mathbf{U}_k$ from $\mathbf{I}$, producing cross-azimuthal coupling which associates more than one element of the receiver and excitation vectors with each singlet frequency. Thus, $a_k^m(t)$ becomes a sum of single harmonics displaying a more complicated temporal behaviour caused by the interchange of energy among azimuthal orders. Since the apparent period of the envelope function is controlled by the singlet frequency perturbations in $\boldsymbol{\Omega}_k$, which are relatively small, $a_k^m(t)$ will be very slowly varying in time.

Provided that a multiplet is approximately uncoupled to any other multiplet, (1) can be used in a variety of ways to model the data. A convenient way to proceed is to linearize equation (1) with respect to the structure coefficients which are themselves linear functionals of aspherical structure (Woodhouse and Giardini, 1985; Ritzwoller et al., 1986). Thus we write

$$
s(\mathbf{r},t) = s_0(\mathbf{r},t) + \sum_{s,t} \frac{\partial s_0(r,t)}{\partial c_s^t} \delta c_s^t + \frac{\partial s_0(\mathbf{r},t)}{\partial \omega_k} \delta\omega_k \tag{10}
$$

Equation (10) is solved iteratively for the δc_s^t in a small frequency band surrounding the mode(s) of interest until a set of c_s^t which adequately predict the spectra are found. These c_s^t may later be used to constrain aspherical structure through inversion of (6). This iterative spectral fitting technique has recently been applied to spectra of resolvably split multiplets from a dataset of recordings from large events (see below). The technique could also be applied to unresolvably split multiplets but we have already seen that rather few parameters are actually required to model the spectra of such multiplets. In fact, for isolated, highly excited fundamental modes, a single resonance function appears to be useful approximation to the observed spectra. To see why this might be so we write equation (1) as

$$
s(\mathbf{r},t) = A(t)\exp(i\omega_k t)
$$

where the real part is understood and

$$
A(t) = \boldsymbol{\sigma}^T \cdot \mathbf{a}(t)
$$

It is straightforward to show that

$$A(t) = A_0 \exp\left[i \int_0^t \frac{\boldsymbol{\sigma}^T \cdot \mathbf{H} \cdot \mathbf{a}(t)}{\boldsymbol{\sigma}^T \cdot \mathbf{a}(t)} \, dt \right] \tag{11}$$

where A_0 is the initial excitation of the multiplet as it would be on a spherical Earth. If we now write

$$\lambda(t) = \frac{\boldsymbol{\sigma}^T \cdot \mathbf{H} \cdot \mathbf{a}(t)}{\boldsymbol{\sigma}^T \cdot \mathbf{a}(t)} \tag{12}$$

we see that $\lambda_0 = \lambda(0)$ is Jordan's location parameter. Equation (1) may now be written

$$s(\mathbf{r},t) = A_0 \exp\left[i \int_0^t \lambda(t) dt \right] \exp(i\omega_k t) \tag{13}$$

If $\lambda(t)$ is only weakly dependent on time, i.e., $\lambda(t) \approx \lambda_0$ then

$$A(t) \approx A_0 \exp(i\lambda_0 t)$$

and (13) becomes

$$s(\mathbf{r},t) \approx A_0 \exp[i(\omega_k + \lambda_0)t] \tag{14}$$

This corresponds to a peak shift in the spectrum which is the asymptotic result of Jordan (1978). Woodhouse and Girnius (1982) give a very elegant analysis of λ_0 and demonstrate that it can be written as a weighted surface integral of aspherical structure. For high l modes, the kernel in the integral is highly oscillatory except in the region of the great circle path joining source and receiver. Thus, in the case of very long wavelength structure, off-path contributions to the integral cancel and λ_0 just becomes sensitive to structure under the great circle path. In fact it is straightforward to show that, in the limit $l \to \infty$ all time derivatives of $\lambda(t)$ are zero so λ is a constant (Dahlen, 1979) and in this limit, the peak shift, λ_0 becomes (Jordan, 1978)

$$\lambda_0 = \frac{\boldsymbol{\sigma}^T \cdot \mathbf{H} \cdot \mathbf{a}(0)}{\boldsymbol{\sigma}^T \cdot \mathbf{a}(0)} \approx \sum_s P_s(0) \sum_t c_s^t \, Y_s^t(\theta,\Phi) \tag{15}$$

where θ, Φ is the location of the pole of the great circle joining the source and receiver. Equation (15) is not very precise in practice, particularly near nodes in the radiation pattern, and several authors have suggested improvements. Davis and Henson (1986) and Romanowicz and Roult (1986) show that to $O(1/l)$ where l is the harmonic degree of a multiplet

$$\lambda_0 = A(l) + \frac{B(l)}{l} \tan((l+\tfrac{1}{2})\Delta - \pi/4 + z) \tag{16}$$

$A(l)$, $B(l)$ and z are source dependent but for an isotropic source $A(l)$ is given by (15) and the second term is the desired correction (Δ is epicentral distance). Romanowicz and Roult (1986) claim that the tangent fluctuations can be sufficiently well measured to provide additional constraints on aspherical structure though it is our experience that the results are sensitive to the peak estimation technique. Davis (1987) avoids using any of the

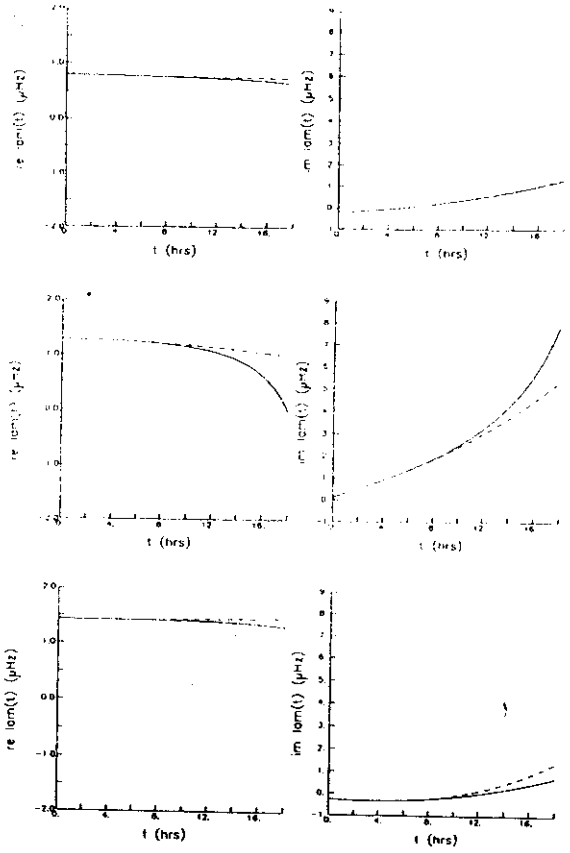

Figure 10. The generalized location parameter, $\lambda(t)$ for ${}_0S_{23}$ (top), ${}_0S_{24}$ (middle) and ${}_0S_{25}$ (bottom) computed for an event in Tonga and recorded at GUMO. The time duration of these plots is what one would typically use in an analysis of these multiplets. Note that $\lambda(t)$ can have quite a strong time dependence with a significant imaginary part. The dashed line is a cubic approximation to $\lambda(t)$. The computations are performed with model M84A.

approximations to λ_0 and uses the definition of $\lambda(0)$ (equation (12)) to relate mode peak measurements to aspherical structure. (This procedure was originally suggested by Jordan (1978)). He finds that degree two structure dominates the peak shifting pattern of fundamental spheroidal modes and otherwise only part of the degree 6 structure is reliably determined. Perhaps one of the reasons for this is that, to order $(1/l)$, more terms appear in the expression for the displacement field because λ cannot be regarded as constant to this level of approximation. A better approximation to (13) might therefore be to let λ be a slowly varying function of time. We write

$$\lambda(t) = \lambda_0 + \frac{d\lambda_0}{dt}\, t + \tfrac{1}{2}\, \frac{d^2\lambda_0}{dt^2}\, t^2 + \cdots \tag{17}$$

so (13) becomes

$$s(\mathbf{r},t) = A_0 \exp\left[i(\lambda_0+\omega_k)t + i \frac{d\lambda_0}{dt}\frac{t^2}{2} + i \frac{d^2\lambda_0}{dt^2}\frac{t^3}{6} + \cdots \right] \tag{18}$$

That (18) might be a reasonable basis for representing the data is demonstrated in Figure 10 where we plot $\lambda(t)$ along with an approximation to it for some fundamental modes calculated using model M84A of Woodhouse and Dziewonski (1984). Note that if rotation and aspherical anelastic structure are neglected, λ_0 is purely real, $d\lambda_0/dt$ is purely imaginary and so on.

It is not immediately apparent how to relate the time domain representation given above to the apparent frequency and attenuation rate measured when fitting a resonance function to the data. Smith et al. (1987) have found that time averages of $\lambda(t)$ give an adequate representation, i.e.,

$$s(\mathbf{r},t) = A_0 \exp(i(\omega_k+\bar{\Lambda})t) \tag{19}$$

where

$$\bar{\Lambda} = \frac{1}{T}\int_0^T w(t)\lambda(t)dt$$

where $w(t)$ is a normalized weight function and T is record length. The measured variation in $\bar{\Lambda}$ can then be related to the splitting matrix and so the c_s^t can be constrained by both measurements of apparent center frequency and attenuation rate.

The above analysis of uncoupled multiplets is relatively complete but a proper treatment of low frequency data requires that we extend the analysis to coupled modes. Loosely speaking, all we need to do is to redefine the vectors in equation (1) to include more than one multiplet and to include in the splitting matrix blocks which describe the interactions of the multiplets. For example if we couple the k and k' multiplets and write

$$\sigma = \begin{bmatrix} \sigma_k \\ \cdots\cdots \\ \sigma_{k'} \end{bmatrix} \qquad \mathbf{a} = \begin{bmatrix} \mathbf{a}_k \\ \cdots\cdots \\ \mathbf{a}_{k'} \end{bmatrix}$$

and

$$\mathbf{H} = \begin{bmatrix} \mathbf{H}_{kk} & \vdots & \mathbf{H}_{kk'} \\ \cdots\cdots & \vdots & \cdots\cdots \\ \mathbf{H}_{k'k} & \vdots & \mathbf{H}_{k'k'} \end{bmatrix}$$

then all the foregoing analysis remains valid. Woodhouse (1980) has provided expressions for the interaction blocks $\mathbf{H}_{kk'}$ in the above formula. These interaction blocks can be written in a similar form to (5) so that the spectrum depends upon an extended set of structure coefficients which can be estimated by iterative spectral fitting. The interaction blocks may have terms depending upon odd-order structure so that the seismograms of coupled multiplets can be weakly dependent on odd-order structure. Recently, expressions for the interaction blocks in H have been extended to include anisotropy and it is now possible to calculate the effect of a small general anisotropic perturbation to a transversely

isotropic reference Earth (Mochizuki, 1986; Tanimoto, 1986b; I. H. Henson, personal communication).

Synthetic seismogram construction including coupling between multiplets has been treated in detail by Tanimoto and Bolt (1983), Morris et al. (1984), and Park and Gilbert (1986). The Galerkin calculation of Park and Gilbert allows probably the most complete treatment of seismic motion on an aspherical Earth and has been used to compare the predictions of some current Earth models with the data (Park, 1986, and below). This calculation is capable of properly coupling modes with very different attenuation rates. This effect is particularly important when coupling spheroidal and toroidal modes together as was first demonstrated by Woodhouse (1980). Along-branch coupling involves modes with very similar Qs so that the Galerkin technique can be replaced with the computationally faster Rayleigh-Ritz technique. The similarity of the radial eigenfunctions of adjacent modes along a branch also allows analytical approximations to be made so that asymptotic forms for coupled mode seismograms can be obtained (Park, 1987; Romanowicz, 1987).

4. Modeling long period data

At frequencies lower than about 6 mHz existing spherically averaged models of elastic structure (e.g., 1066A, Gilbert and Dziewonski, 1975; PREM, Dziewonski and Anderson, 1981), and attenuation structure (Masters and Gilbert, 1983; Masters et al., 1983) are sufficiently accurate to allow retrieval of a reliable source mechanism. We have found that, at these frequencies, the source can be adequately characterized by the six elements of the "seismic moment tensor" and a source time function. This latter feature is necessary to account for the fact that the low frequency centroid time of the event is not necessarily the same as the origin time deduced from body wave arrivals (Backus, 1977; Dziewonski and Woodhouse, 1983). The exact form of the source time function is not important as far as the quality of the fit to the data in this frequency band is concerned. We have also found that mislocation of the spatial centroid of the event does not significantly degrade the fit to the data in this frequency band though it is possible to find an optimum location (Dziewonski et al., 1981). Source retrieval is, in principle, a straightforward operation (e.g., Buland and Gilbert, 1976) though linear fitting for the elements of the seismic moment tensor does not always succeed. The main problem is phase mismatching due to the presence of aspherical structure leading to a bias toward low moment. This bias can be reduced by modifying the source orientation to predict, as best as possible, the observed distribution of power at all stations recording the event. The moment tensors used to calculate the synthetic seismograms of Figure 2 were obtained with this technique.

Despite the perturbing influence of aspherical structure, our fit to the long period data is sufficiently good that we are encouraged to use the multiplet stacking and stripping techniques described by Gilbert and Dziewonski (1975) to improve our estimates of multiplet degenerate frequencies. Such measurements can then be used to improve our models of spherically averaged structure (the "terrestrial monopole"). We rewrite equation (1) in the frequency domain, i.e.,

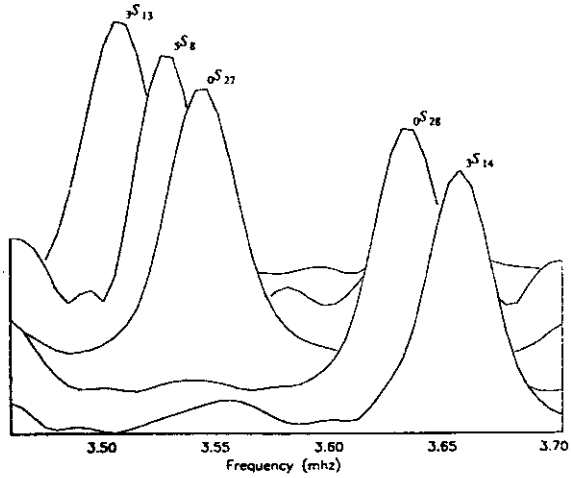

Figure 11. The results of stripping 800 recordings in a small frequency band which includes the fundamental spheroidal modes ${}_0S_{27}$ and ${}_0S_{28}$. Each "row" of the figure is the amplitude spectrum of a single $c_k(\omega)$. Note that overtones such as ${}_3S_{14}$ are clearly separated from the highly excited fundamental modes.

$$s_j(\omega) = \sum_{k=1}^{K} A_{jk}(\omega)\, C_k(\omega) \tag{20}$$

where $C_k(\omega)$ is the resonance function of the kth mode (i.e., the spectrum of a decaying cosinusoid). A_{jk} is the complex amplitude of the kth mode recorded at the jth station which may be estimated if we have a model of the source and a provisional model of Earth structure. Equation (20) can be solved for the $C_k(\omega)$ in a small frequency band incorporating K modes if we have K or more recordings. Typically we will have several hundred recordings so the multiplet resonance functions can be recovered (Figure 11). Frequency and attenuation can now be estimated from the isolated resonance functions.

Multiplet stacking and stripping only gives unbiased degenerate frequencies when the multiplet in question has a relatively uniform frequency distribution of singlets. When a multiplet has a highly nonuniform distribution of singlets or its singlets are nonuniformly excited, stripping fails by giving a peak at a subset of the singlets which may have a very different frequency from the true degenerate frequency. Diagnosis of such a failure may be difficult but a common symptom is for the strip to have multiple peaks. For example, multiplet stacking and stripping is incapable of producing accurate results for broadly split modes such as ${}_1S_4$. The situation is even worse for anomalously split low l, high Q modes such as ${}_{10}S_2$ where multiplet stripping produces a single peak at an extreme end of the multiplet leading to systematically biased degenerate frequencies.

Ritzwoller et al. (1986, 1987) demonstrate that accurate degenerate frequencies for broadly split multiplets can be found by either stripping for individual singlets or by directly modeling the effect of aspherical structure on the data spectra. Equation (20) can be modified in a straightforward way to strip for individual singlets within a multiplet provided that a reasonably accurate estimate of the singlet eigenvectors is known. For example, it is reasonable to suppose that, for rotationally dominated modes like ${}_1S_4$, the splitting matrix is diagonally dominant. If this is true, U in equation (9) is the unit matrix so that (9) can be written in exactly the same form as (1) and we are able to calculate the

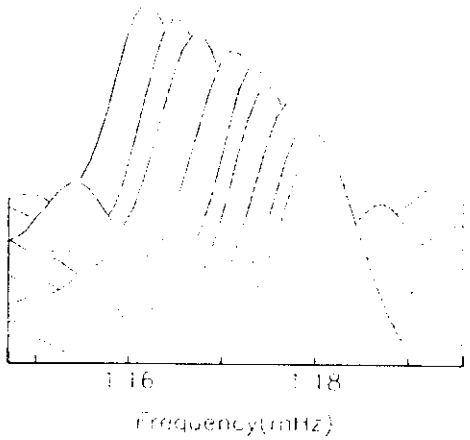

Figure 12. This figure has the same format as Figure 11 but now each row is the amplitude spectrum of a singlet of ${}_1S_4$. All nine singlets are recovered and follow a quadratic in azimuthal order close to that predicted for a rotating, hydrostatic Earth model.

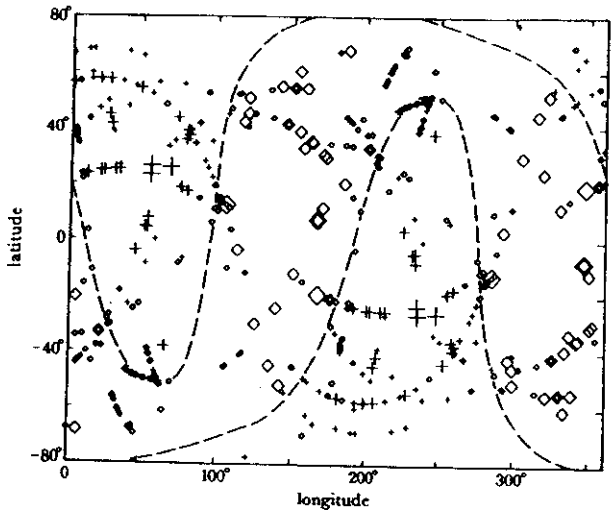

Figure 13. The effect of aspherical structure on center frequency can be seen by plotting the shift in frequency as a function of the pole position of the great circle joining source and receiver. Each symbol is plotted at a pole position: a + corresponds to a positive frequency shift and a <> corresponds to a negative frequency shift. The size of the symbol is indicative of the magnitude of the shift: the smallest symbols correspond to a 0–0.1% shift and the largest to a 0.3–0.4% shift. A degree-two spherical harmonic pattern accounts for most of the structure in the observations; the nodal lines of this pattern are shown by the dashed lines. This example is a combination of measurements for the modes ${}_0S_{21} - {}_0S_{23}$.

excitations of individual singlets. We may then stack or strip recordings to enhance desired singlets. It turns out that we are able to recover all the singlet resonance functions of ${}_1S_4$ (Figure 12) and so estimate a precise degenerate frequency (i.e., by employing the diagonal sum rule [Gilbert, 1971]).

Even when singlets within a multiplet are uniformly distributed, multiplet stripping can still give biased measurements due to inadequate geographical sampling of the Earth. The exact location of the center frequency of a recovered resonance function will depend upon

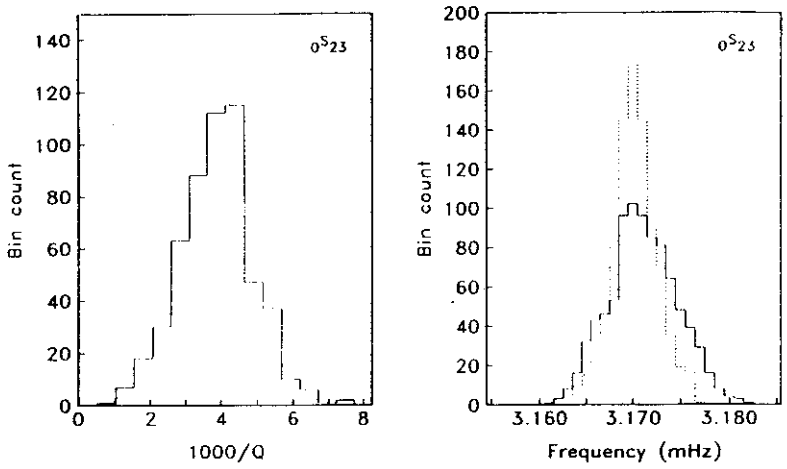

Figure 14. Histograms of $1000/Q$ and center frequency measurements obtained by fitting a decaying cosinusoid model to many spectra of the multiplet $_0S_{23}$. The effect of removing the frequency shifts due to a dominant degree 2 elastic aspherical structure is shown by the dashed line in the right-hand figure. No large scale structure is visible in the attenuation data.

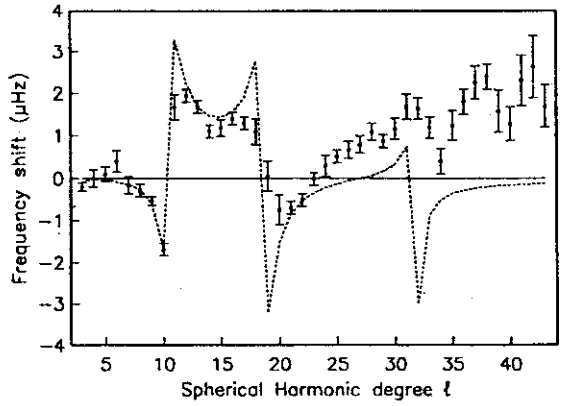

Figure 15. Observed degenerate frequencies of fundamental spheroidal modes presented as frequency shifts from the predictions of model 1066A. The discontinuous nature of the observations is mimicked by a calculation of the perturbing effect of Coriolis coupling to nearby toroidal modes (dashed line). Model 1066A systematically misfits the observations for $l \geq 25$.

the choice of records employed in the analysis. If a mode is sufficiently well isolated and of sufficiently high amplitude that its properties can be measured from individual recordings, we may analyze the geographical peak shifting effect directly. This was the approach taken by Masters et al. (1982) and, more recently (and with less assumptions), by Davis (1987). Equation (15) suggests that, if the asymptotic limit is valid, the magnitude of a peak frequency shift should be a smooth function of the pole position of the great circle joining the source and receiver. If we plot the raw measurements in this way (Figure 13), we find that a simple pattern emerges from the data which is dominantly of harmonic degree two. This pattern persists for fundamental spheroidal modes over a large range of l though by $l \geq 43$ (i.e., periods shorter than 200 secs) the degree 2 pattern is no longer as

dominant. It should be noted that, if we use the asymptotic formula (15) to interpret peak shift data we can only reliably determine the large degree 2 structure and even this is subject to some bias. The signal from higher order structure is sufficiently small (at least at periods longer than about 200 seconds) that we must use the full expression for λ which includes off-path propagation effects. It is unlikely that the great circle approximation improves at shorter periods. Histograms of the results of single station peak analysis are shown in Figure 14.

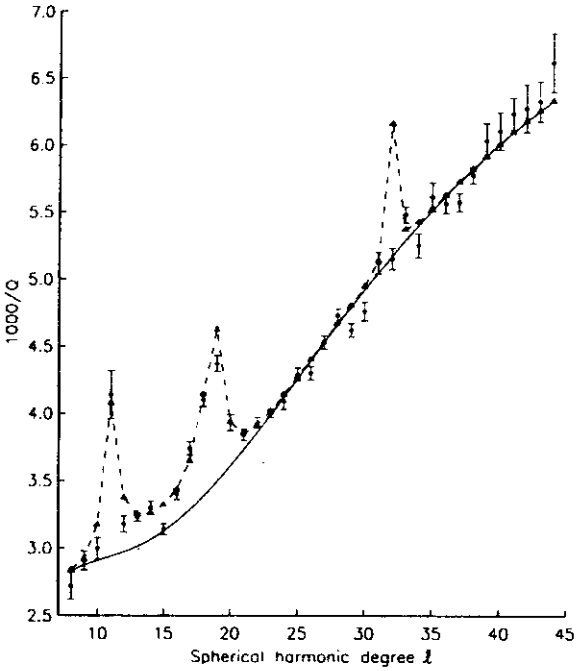

Figure 16. Observed mean attenuation rates of fundamental spheroidal modes. The dashed line again shows the predicted effect of Coriolis coupling and follows the data for $l \lesssim 25$. The predicted strong coupling at $l \approx 32$ is absent in the data (see text).

The spread in center frequency estimates is dominantly controlled by large-scale aspherical structure. Removal of the effect of a dominant degree 2 elastic structure greatly reduces the variance in the frequency observations. The spread in apparent attenuation measurements is too large to be ascribed to aspherical attenuation structure and is dominantly due to interference effects. Davis (1985) shows that the observed spread in apparent attenuation can be generated solely by elastic aspherical structure and it is likely that true aspherical attenuation structure constitutes only a small part of the signal. Davis (1987) reports that part of the degree 6 structure can also be reliably determined from peak shift data (as well as the degree 2 structure) provided the full expression for $\lambda(0)$ is used. He also notes that there is still signal remaining in the peak shift data which may be partly due to the fact that $\lambda(0)$ is not precisely the same as the observed peak shift (see equation (18) for a better approximation). The analysis also neglects multiplet/multiplet coupling which certainly contributes to the observed signal where Coriolis coupling is known to occur but may also contribute because of along-branch coupling (see below).

Accurate estimates of fundamental spheroidal mode degenerate frequencies from the analysis of peak shift patterns are shown in Figure 15. The frequencies are not a smooth function of harmonic degree and the "tears" observed at $l = 11$ and 19 are due to strong

Coriolis coupling to ${}_0T_{12}$ and ${}_0T_{20}$ respectively. A coupling calculation using the Galerkin technique described by Park and Gilbert (1986) shows that, unless coupling is extremely strong, the singlets of a coupled ${}_0S_l - {}_0T_{l+1}$ pair fall into two groups, one with dominantly spheroidal characteristics, the other with dominantly toroidal characteristics. The frequencies of the singlets within each group are repelled so that, on average, the multiplets appear to be further apart than when they are uncoupled. The attenuations, on the other hand, are averaged so that coupled singlets which are dominantly spheroidal are more quickly attenuated than uncoupled spheroidal mode singlets. This latter feature is illustrated in Figure 16 where mean attenuation rates for spheroidal modes (or the dominantly spheroidal part of a spheroidal/toroidal coupled pair) are shown along with a prediction of the effect of coupling. The strong coupling calculated at harmonic degree 32 occurs because ${}_0S_{32}$ and ${}_0T_{31}$ have frequencies separated by only 0.6 μHz in model 1066A of Gilbert and Dziewonski (1975). This predicted strong coupling is a feature of most modern models but is absent in the data because ${}_0S_{32}$ and ${}_0T_{31}$ are actually separated by about 10 μHz in degenerate frequency which is sufficient to significantly reduce the strength of coupling. This sensitivity of coupling calculations to the frequency separation of multiplets highlights the importance of having more accurate spherically averaged Earth models than are currently available.

It is difficult to extend the peak shift analysis to higher frequencies unless measurements of the center frequencies of several adjacent modes are made simultaneously. Another way to proceed is to use surface wave dispersion analysis. This has been the approach of Nakanishi and Anderson (1983, 1984) who have estimated phase velocity from Rayleigh and Love wave packets which have traveled through a great circle and have also made single station phase and group velocity measurements between 100- and 300-sec periods. These authors have performed a spherical harmonic analysis of their data assuming that the observed phase shifts represent line integral averages over the minor arc from source to receiver and over great circles. Inspection of their results shows that odd-order structure is poorly resolved by the data and only a few of their spherical harmonic coefficients are significant at the 95% confidence level. A formal resolution analysis by Tanimoto (1985) demonstrates that this dataset constrains little of the geographical variation in phase velocity at the 95% confidence level. This result is a little disappointing, especially if one remembers that no off-path propagation has been accounted for in the analysis and that the assessment of data errors is quite subjective. The neglect of off-path propagation has been justified by invoking Fermat's principle which tells us that errors in the phase will be of second order if we ignore path perturbations and great circle wave propagation has also been assumed by Woodhouse and Dziewonski (1984) in their waveform fitting experiment. They showed that the difference in phase anomaly accumulated along a great circle and minor arc can be represented by a fictitious shift in the epicentral distance. This clever observation allowed them to efficiently construct differential seismograms for both even- and odd-order structure components. Their differential seismograms included overtone contributions but the dominance of the fundamental modes in the data means that this is largely the signal that is being fit.

The availability of a model like M84A allows us to test the various approximations that are used in modeling aspherical structure. Park (1986) has used this model to construct synthetic seismograms using various coupling schemes. He finds that the addition of

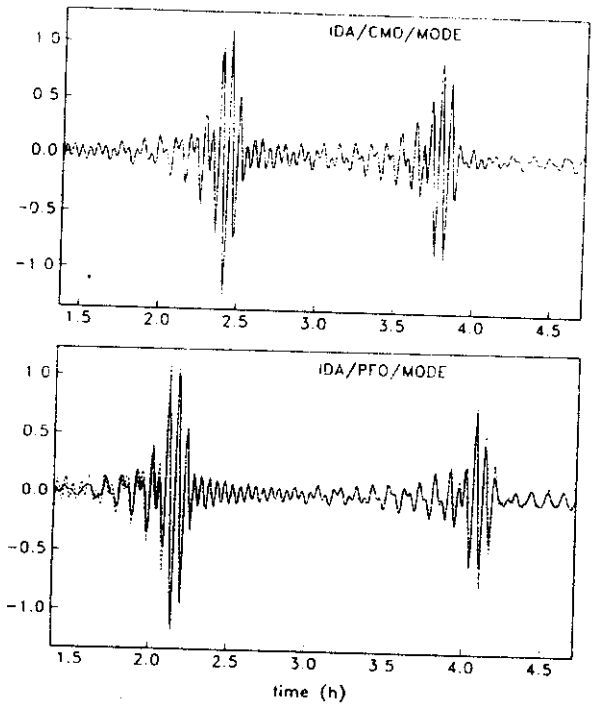

Figure 17. Comparisons of along-branch fundamental spheroidal mode coupled synthetic seismograms (solid line) with uncoupled synthetic seismograms (dashed line). All fundamental modes with frequencies less than 6 mHz are included and nearest neighbor coupling is calculated using model M84A for the event in Iran, 1978/259. The difference between the synthetics is the effect of odd-order structure. In most cases the differences are extremely small but occasionally, amplitude and phase anomalies are visible (e.g., PFO).

along-branch coupling (so giving sensitivity to odd-order structure) causes very small additional perturbations to the seismograms at long periods. In fact the phase shift induced by odd-order structure is of the same order of magnitude as the error in the phase shift incurred by neglecting off-path propagation. We illustrate the additional signal from the odd-order structure of M84A by comparing uncoupled and along-branch coupled fundamental mode synthetics in Figures 17 and 18. The calculations include only nearest-neighbor fundamental spheroidal mode coupling up to a frequency of 6 mHz. The synthetics are computed for an Iranian earthquake (1978/259) which was extremely shallow and so is dominated by fundamental mode energy. A typical comparison is given by the station CMO with almost no difference in the time or frequency domain between uncoupled and coupled synthetics. One of the largest computed differences is shown by station PFO in which R_2 is phase shifted by several seconds and the amplitude spectra are strongly perturbed. Comparison of such coupled mode synthetic seismograms with the data demonstrates that much of the signal is not modeled. In particular, mode amplitudes (and surface wave amplitude anomalies in the time domain) are not well fit. The general impression is that the current models underpredict the magnitude of the anomalies and higher-order structure will probably be required to match the data. Another conclusion that

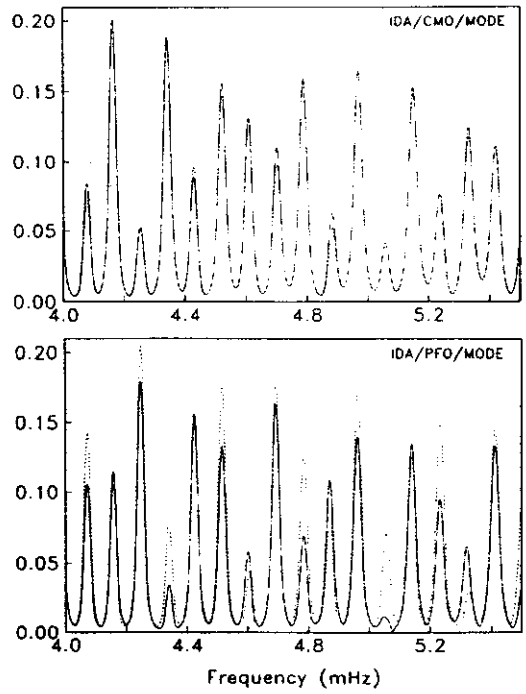

Figure 18. Comparisons of Hanning tapered spectra of 25-hour recordings with and without the effects of along-branch coupling (see Figure 17 caption for details). Most spectral comparisons are like CMO where large differences are only seen near excitation nodes. PFO shows quite large amplitude perturbations.

we can draw is that the current models predict basically no effect of odd-order structure via along-branch coupling on low-frequency peak shifts or apparent attenuation rates (Figure 19) so it is unlikely that this will account for our present inability to model these data.

Clearly, we do not yet have an aspherical model which gives a reliable prediction o surface wave propagation. In any case, the models we have been discussing ar dominantly controlled by fundamental modes which are only sensitive to structure in th upper mantle. The depth resolution of fundamental modes is notoriously poor and a forma analysis by Tanimoto (1986a) shows that vertical resolving lengths are of the order of two hundred kilometers or more. To improve this we must add overtone information or, if w are performing waveform fits, the overtone wave packets must be given additional weigh to compete with the larger amplitude fundamental modes (e.g., Tanimoto, 1987). As note earlier in this paper we do have some observations of split overtone multiplets and we no discuss the current interpretation of these data. Ritzwoller et al. (1987) and Giardini et a (1987) have both analyzed a similar set of about 40 multiplets and recovered the c structure coefficients for harmonic degrees $s=2$ and 4. An example of the ability c iterative spectral fitting to fit the data is shown in Figure 20. Roughly ten of thes multiplets are anomalously split, all of which sample the core. For most multiplet Ritzwoller et al. (1987) find that only the c_2^t are significant and simple aspherical structur in the mantle are capable of explaining most of the observations. What these models do n explain are the c_2^0 coefficients of the anomalously split multiplets. We require son perturbation in core structure to fit these data. Improvements can be achieved by t inclusion of any of the following structures: isotropic perturbations in the inner or out

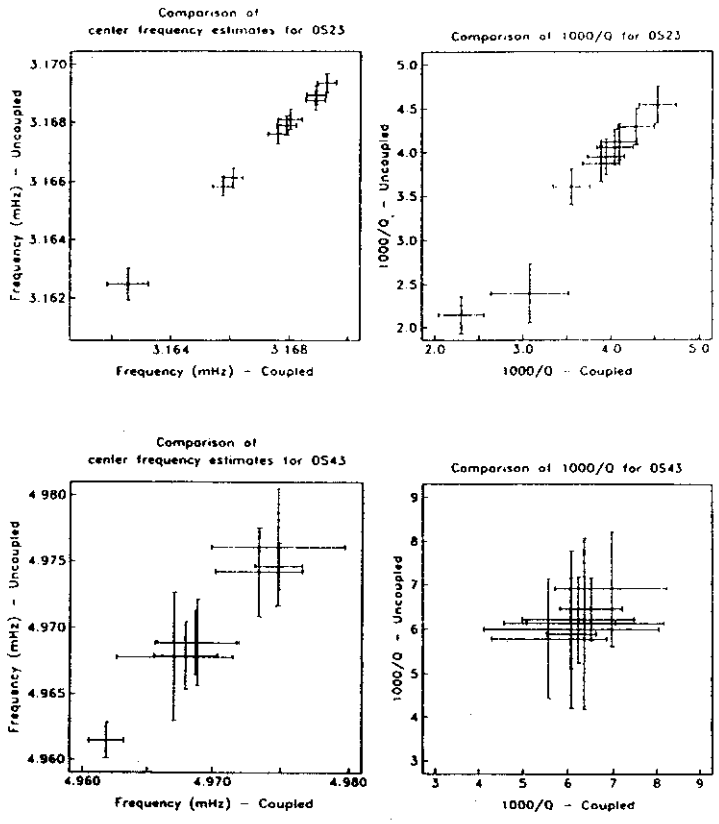

Figure 19. A comparison of center frequency and attenuation estimates for ${}_0S_{23}$ (upper panels) and ${}_0S_{43}$ (lower panels) made from synthetic seismograms with and without along-branch coupling (see Figure 17 caption). These results indicate that this type of coupling has little effect on such estimates.

core, perturbations to the boundaries of the fluid outer core and also, apparently, anisotropic perturbations to the inner core (Woodhouse et al., 1986). This last structure is the only one on this list which appears to allow the very anomalously split but poorly excited multiplet ${}_3S_2$ to be fit. However, the amount of anomalous structure in these models is extremely large and a definitive solution has yet to be found.

5. Conclusions

Aspherical Earth structure manifests itself in long period seismic data in many ways through the splitting and coupling of multiplets. Nearly all research to date has concentrated on either the highly excited fundamental modes or on low harmonic degree, high Q overtones. Fundamental modes show peak shifting and anomalous attenuation rates in the frequency domain and phase perturbation and amplitude anomalies of surface wave

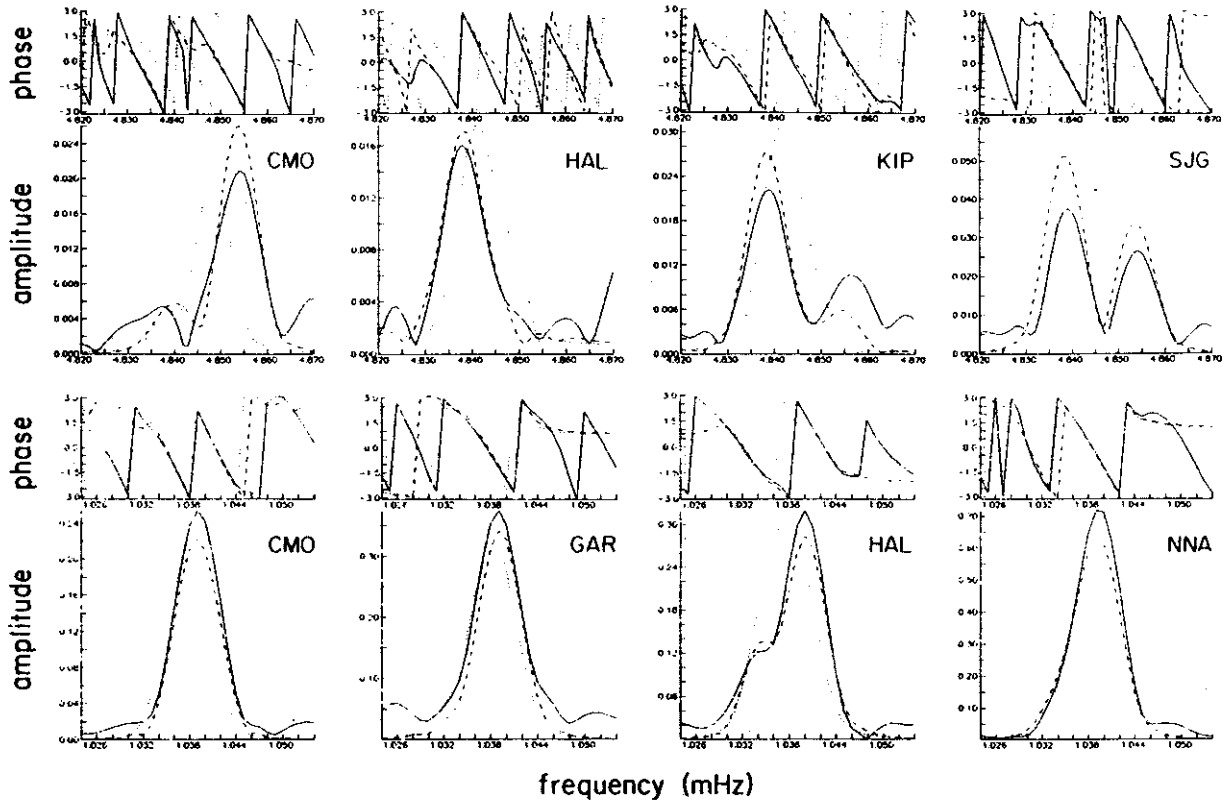

Figure 20. Amplitude and phase spectra showing the fit to the data (solid line) of a rotating hydrostatic Earth model (dotted line) and of a model which includes c_2^1 and c_4^1 coefficients (dashed line). The rotating hydrostatic Earth model is incapable of fitting the data (note that agreement in phase can only occur when peaks are above the noise). The upper figures show spectra of the mode ${}_{13}S_2$ computed using 60-hour recordings of the Banda Sea event (1982/173). The lower figures show spectra of the mode ${}_0S_6$ computed using 90-hour recordings of the Sumbawa event (1977/231). All time series were recorded on the IDA array.

packets in the time domain. Also clearly visible in the frequency band 1.5–3 mHz is Coriolis coupling between spheroidal and toroidal modes. Peak shifting measurements are mainly restricted to fundamental modes of periods longer than 200 sec because of the difficulty of identifying isolated multiplets on single recordings at shorter periods. The peak shifting pattern is dominated by a degree 2 pattern with some resolvable degree 6 structure. Current analyses of the peak shift data include nonasymptotic effects though neglect multiplet/multiplet coupling. Synthetic seismogram experiments indicate that along-branch coupling has little effect on peak frequency measurements. Surface wave phase velocity perturbations have, until now, been interpreted in a pure-path framework where off-path propagation is ignored. Synthetic experiments indicate that the error induced by this approximation can rival the weak signal from odd-order structure so that the odd-order part of the model may be suspect. Woodhouse and Dziewonski's (1984) models predict that the power in degrees 2 and 6 structure exceeds that in degrees 4 and 8 showing some consistency with the peak shifting results though the agreement of the structure coefficients is quite poor. Agreement of the peak shifting and waveform fitting experiments with the dispersion models of Nakanishi and Anderson (1983, 1984) is also

poor. This is particularly true at long periods suggesting that the dispersion analyses are unreliable at periods longer than about 250 sec.

The lack of agreement of results described above is probably not surprising given the fact that these models are the first real attempts at constraining global aspherical structure. These models provide a first chance to construct accurate synthetic seismograms and see if classical approximations (such as the pure path approximation) are useful. The results indicate that more accurate theoretical formulations must be used in the inversion process if we are to recover reliable models of aspherical structure. It is probably also true that we will need to be more sophisticated in our analysis of surface wave dispersion if we are to get precise enough data to usefully constrain large-scale structure. In particular, ways of reliably assigning observational errors to dispersion data are needed so that we can have confidence in the resulting models.

The analysis of overtones, including that of the anomalously split multiplets, has provided some reliable estimates of structure coefficients, c_s^t, which in principle are sensitive to structure throughout the Earth. Unfortunately there are insufficient observations to independently constrain deep Earth structure though some progress appears to have been made by combining these data with constraints from the ISC dataset (Giardini et al., 1987). One thing is clear, the retrieval of aspherical Earth structure from low frequency seismic data will remain a fertile area of research for many years to come.

6. Acknowledgments

We gratefully acknowledge the help of Freeman Gilbert, Ivan Henson, Mark Smith, and Rudolf Widmer. Rudy's help in making pictures went above and beyond the call of duty. We also wish to thank those people who responded to our request for information. The revised scope of this paper made it impossible to properly survey the field and we hope to do this in a later contribution. Thanks are due to the operators of the IDA, GDSN and GEOSCOPE networks for their continued efforts to maintain the high quality of digital data and a special thanks to Cecil H. and Ida Green for their past and continued support of the IDA network. This research was supported by National Science Foundation grants EAR-84-10369 and EAR-84-18471.

References

Agnew, D., J. Berger, R. Buland, W. Farrell, and F. Gilbert (1976). International deployment of accelerometers: A network for very long period seismology, *Eos*, 57, 180-188.

Agnew, D. C., J. Berger, W. E. Farrell, J. F. Gilbert, G. Masters, and D. Miller (1986). Project IDA: A Decade in review, *Eos*, 67, 203-212.

Backus, G. E. (1977). Seismic sources with observable glut moments of spatial degree two, *Geophys. J. R. Astron. Soc.*, 51, 27-45.

Backus, G. E., and F. Gilbert (1961). Rotational splitting of the free oscillations of the earth, *Proc. Natl. Acad. Sci.*, 47, 362-371.

Benioff, H., F. Press, and S. W.Smith (1961). Excitation of the free oscillations of the earth by earthquakes, *J. Geophys. Res.*, 66, 605-619.

Buland, R., and F. Gilbert (1976). Matched filtering for the seismic moment tensor, *Geophys. Res. Ltrs.*, 3, 205-

206.

Dahlen, F. A. (1968). The normal modes of a rotating, elliptical earth, *Geophys. J. R. Astron. Soc.*, 16, 329-367.

Dahlen, F. A. (1969). The normal modes of a rotating, elliptical earth, II, Near resonance multiplet coupling, *Geophys, J. R. Astron. Soc.*, 18, 397-436.

Dahlen, F. A. (1979). The spectra of unresolved split normal mode multiplets, *Geophys. J. R. Astron. Soc.*, 58, 1-33.

Dahlen, F. A. (1982). The effect of data windows on the estimation of free oscillation parameters, *Geophys. J. R. Astron. Soc.*, 69, 537-549.

Dahlen, F. A., and R. V. Sailor (1979). Rotational and elliptical splitting of the free oscillations of the earth, *Geophys. J. R. Astron. Soc.*, 58, 609-623.

Davis, J. P. (1985). Variation in apparent attenuation of the earth's normal modes due to lateral heterogeneity, *Geophys. Res. Lett.*, 12, 141-143.

Davis, J. P. (1987). Local eigenfrequency and its uncertainty inferred from fundamental spheroidal mode frequency shifts, *Geophys. J. R. Astron. Soc.*, 88, 693-722.

Davis, J. P., and I. H. Henson (1986). Validity of the great circular average approximation for inversion of normal mode measurements, *Geophys. J. R. Astron. Soc.*, 85, 69-92.

Dziewonski, A. M., and D. Anderson (1981). Preliminary reference Earth model, *Phys. Earth Planet. Inter.*, 25, 297-356.

Dziewonski, A. M., and J. Steim (1982). Dispersion and attenuation of mantle waves through wave-form inversion, *Geophys. J. R. Astron. Soc.*, 70, 503-527.

Dziewonski, A. M., T. A. Chou, and J. H. Woodhouse (1981). Determination of earthquake source parameters from waveform data for studies of global and regional seismicity, *J. Geophys. Res.*, 36, 2825-2831.

Dziewonski, A. M., and J. H. Woodhouse (1983). Studies of the seismic source using normal mode theory, in *Earthquakes: Observation, Theory and Interpretation*, pp45-137. edited by E. Boschi and H. Kanamori.

Edmonds, A. R. (1960). *Angular Momentum and Quantum Mechanics*, Princeton University Press, Princeton, NJ.

Fichler, C., M. Grünewald, and W. Zürn (1986). Observation of spheroidal-toroidal mode coupling, *Ann. Geoph.*, 4B, 251-260.

Giardini, D., X.-D. Li, and J. H. Woodhouse (1987). Three-dimensional structure of the earth from splitting in free oscillation spectra, *Nature*, 325, 405-409.

Gilbert, F. (1970). Excitation of the normal modes of the Earth by earthquake sources, research note, *Geophys. J. R. Astron. Soc.*, 22, 223-226.

Gilbert, F. (1971). The diagonal sum rule and averaged eigenfrequencies, *Geophys. J. R. Astron. Soc.*, 23, 119-123.

Gilbert, F., and A. Dziewonski (1975). An application of normal mode theory to the retrieval of structural parameters and source mechanisms from seismic spectra, *Philos. Trans. R. Soc. London Ser. A*, 278, 187-269.

Harris, F. (1978) On the use of windows for harmonic analysis with the discrete Fourier transform, *Proc. IEEE*, 66, 51-83.

Jenkins, G. M., and D. G. Watts (1968). *Spectral Analysis and its Applications*, Holden-Day, pp. 525.

Jordan, T. H. (1978). A procedure for estimating lateral variations from low-frequency eigenspectra data, *Geophys. J. R. Astron. Soc.*, 52, 441-455.

Lay, T., and H. Kanamori (1985). Geometric effects of global lateral heterogeneity on long-period surface wave propagation, *J. Geophys. Res.*, 90, 605-621.

Lindberg, C. L. (1986). Multiple taper spectral analysis of terrestrial free oscillations, Ph.D. Thesis, Univ. of California, San Diego.

Luh, P. C. (1973). Free oscillations of the laterally inhomogeneous earth: Quasi degenerate multiplet coupling, *Geophys. J. R. Astron. Soc.*, 32, 187-202.

Luh, P. C. (1974). The normal modes of the rotating self gravitating inhomogeneous earth, *Geophys. J. R. Astron. Soc.*, 38, 187-224.

Masters, G., T. H. Jordan, P. G. Silver, and F. Gilbert (1982). Aspherical earth structure from fundamenta spheroidal-mode data, *Nature*, 298, 609-613.

Masters, G., J. Park, and F. Gilbert (1983). Observations of coupled spheroidal and toroidal modes, *J. Geophys Res.* 88, 10,285-10,298.

Masters, G., and F. Gilbert (1983). Attenuation in the earth at low frequencies, *Philos. Trans. R. Soc. London Ser A*, 308, 479-522.

Morris, S. P., H. Kawakatsu, R. J. Geller, and S. Tsuboi (1984). A calculation of the normal modes of realistic laterally heterogeneous, anelastic earthmodels at 250 sec period, *Eos Trans AGU*, **65**, 1002.

Nakanishi, I. (1979). Phase velocity and Q of mantle Rayleigh waves, *Geophys. J. Roy. Astron. Soc.*, **58**, 35-59.

Nakanishi, I., and D. Anderson (1983). Measurements of mantle wave velocities and inversion for lateral heterogeneity and anisotropy. I. Analysis of great-circle phase velocities, *J. Geophys. Res.*, **88**, 10-267.

Nakanishi, I., and D. Anderson (1984). Measurements of mantle wave velocities and inversion for lateral heterogeneity and anisotropy. II. Analysis by the singlet station method, *Geophys. J. R. Astron. Soc.*, **78**, 573-617.

Nataf, H.-C., I. Nakanishi, and D. L. Anderson (1986). Measurements of mantle wave velocities and inversion for lateral heterogeneities and anisotropy, 3. Inversion, *J. Geophys. Res.*, **91**, 7261-7307.

Ness, N. F, C. J. Harrison, and L. J. Slichter (1961). Observations of the free oscillations of the earth, *J. Geophys. Res.*, **66**, 621-629.

Niazi, M., and H. Kanamori (1981). Source parameters of 1978 Tabas and 1979 Quainat, Iran, earthquakes from long period surface waves, *Bull. Seismol. Soc. Am.*, **71**, 1201-1213.

Park, J. (1986). Synthetic seismograms from coupled free oscillations: The effects of lateral structure and rotation, *J. Geophys. Res.*, **91**, 6441-6464.

Park, J. (1987). Asymptotic coupled-mode expressions for multiplet amplitude anomalies and frequency shifts on a laterally heterogeneous Earth, *Geophys. J. R. Astron. Soc.* (in press).

Park, J., and F. Gilbert (1986). Coupled free oscillations of an aspherical dissipative rotation earth: Galerkin theory, *J. Geophys. Res.*, **91**, 7241-7260.

Pekeris, C. L., A. Alterman, and M. Jarosch (1961). Rotational multiplets in the spectrum of the earth, *Phys. Rev.*, **122**, 1692-1700.

Peterson, J., C. R. Hutt, and L. G. Holkomb (1980). Test and calibration of the SRO observations, U.S.G.S. report.

Ritzwoller, M., G. Masters, and F. Gilbert (1986). Observations of anomalous splitting and their interpretation in terms of aspherical structure, *J. Geophys. Res.*, **91**, 10,203-10,228.

Ritzwoller, M., G. Masters, and F. Gilbert (1987). Constraining aspherical structure with low frequency interaction coefficients: Application to uncoupled multiplets, *J. Geophys. Res.*, in review.

Romanowicz, B. (1987). Multiplet-multiplet coupling due to lateral heterogeneity: asymptotic effects on the amplitude and frequency of the Earth's normal modes, *Geophys. J. R. Astron. Soc.* (submitted).

Romanowicz, B., and G. Roult (1986). First order asymptotics for the eigenfrequencies of the Earth and application to the retrieval of large scale lateral variations of structure, *Geophys. J. Roy. Astron. Soc.*, **87**, 209-239.

Romanowicz, B., M. Cara, J. F. Fels, and G. Roult (1984). GEOSCOPE; a French initiative in long period three component global seismic networks, *Eos Trans. AGU*, **65**, 753-756.

Schulten, K., and R. Gordon (1975). Exact recursive evaluation of $3{-}j$ and $6{-}j$ coefficients for quantum mechanical coupling of angular momenta, *J. Math. Phys.*, **16**, 1961-1870.

Slepian, D. (1978). Prolate spheroidal wave functions, Fourier analysis, and uncertainty. V: The discrete case, *Bill Systems Tech. J.*, **57**, 1371-1430.

Smith, M. F., G. Masters, and M. Ritzwoller (1987). Constraining aspherical structure with normal mode frequency and attenuation measurements, *Eos Trans. AGU*, **68**, 358.

Tanimoto, T. (1985). The Backus-Gilbert approach to the three-dimensional structure in the upper mantle, I., Lateral variation of surface wave phase velocity with its error and resolution, *Geophys. J. R. Astron. Soc.*, **82**, 105-124.

Tanimoto, T. (1986a). The Backus-Gilbert approach to the three-dimensional structure in the upper mantle, II, SH and SV velocity, *Geophys. J. R. Astron. Soc.*, **84**, 49-70.

Tanimoto, T. (1986b). Free oscillations in a slightly anisotropic earth, *Geophys. J. R. Astron. Soc.*, **87**, 493-517.

Tanimoto, T. (1987). The three-dimensional shear wave structure in the mantle by overtone waveform inversion — 1. Radial seismogram inversion, *Geophys. J. R. Astron. Soc.*, **89**, 713-740.

Tanimoto, T., and B. A. Bolt (1983). Coupling of torsional modes in the earth, *Geophys. J. R. Astron. Soc.*, **74**, 83-96.

Thomson, D. J. (1982). Spectrum estimation and harmonic analysis, *IEEE Proc.*, **70**, 1055-1096.

Wielandt, E., and G. Streckheisen (1982). The leaf spring seismometer: design and performance, *Bull. Seismol. Soc. Am.*, **72**, 2349-2368.

Woodhouse, J. H. (1980). The coupling and attenuation of nearly resonant multiplets in the earth's free oscillation spectrum, *Geophys. J. R. Astron. Soc.*, **61**, 261-283.

Woodhouse, J. H., and F. A. Dahlen (1978). The effect of a general aspherical perturbation on the free oscillations of the earth, *Geophys. J. R. Astron. Soc.*, 53, 335-354.

Woodhouse, J. H., and A. M. Dziewonski (1984). Mapping of the upper mantle: three-dimensional modeling of earth structure by inversion of seismic waveforms, *J.Geophys. Res.*, 89, 5953-5986.

Woodhouse, J. H., and D. Giardini (1985). Inversion for the splitting function of isolated low order normal mode multiplets, *Eos Trans. AGU*, 66, 300.

Woodhouse, J. H., and T. P. Gimius (1982). Surface waves and free oscillations in a regionalized earth model, *Geophys. J. R. Astron. Soc.*, 68, 653-673.

Woodhouse, J. H., and Y. K. Wong (1986). Amplitude, phase and ray anomalies of mantle waves, *Geophys. J. Roy. Astron. Soc.*, 87, 753-773.

Woodhouse, J. H., D. Giardini, and X.-D. Li (1986). Evidence for inner core anisotropy from free oscillations, *Geophys. Res. Lett.*, 13, 1549-1552.

G. MASTERS and M. RITZWOLLER, Institute of Geophysics and Planetary Physics, University of California, San Diego, La Jolla CA 92093, USA.